JAAS

Cite this: *J. Anal. At. Spectrom.*, 2012, **27**, 310

www.rsc.org/jaas

PAPER

Determination of Fe^{2+} and Fe^{3+} species by FIA-CRC-ICP-MS in Antarctic ice samples†

Andrea Spolaor,[ab] Paul Vallelonga,[cd] Jacopo Gabrieli,[d] Giulio Cozzi,[d] Claude Boutron[f] and Carlo Barbante*[bde]

Received 17th September 2011, Accepted 1st November 2011
DOI: 10.1039/c1ja10276a

Iron is an element of great interest due to its role in primary production and in oceanic carbon cycle regulation, such that past changes in iron deposition may have influenced oceanic sequestration of atmospheric CO_2 on millennial time scales. The behavior of iron in biological and environmental contexts depends strongly on its oxidation state. Solubility in water and the capacity to form complexes are just two important characteristics that are species dependent. Distinguishing between the two iron species, Fe(II) and Fe(III), is necessary to evaluate bioavailability, as Fe(II) is more soluble and therefore more readily available for phytoplankton uptake and growth. Here, we present a novel analytical method for iron speciation analysis using Collision Reaction Cell-Inductively Coupled Plasma-Mass Spectrometry (CRC-ICP-MS) and apply it to ice core samples from Talos Dome, Antarctica. The method detection limit is 0.01 ng g^{-1}. A chelating resin, Ni-NTA Superflow, was used to separate the Fe species. At pH 2 the resin is capable of retaining Fe^{3+} with no retention of Fe^{2+}. After the initial separation, we oxidized the Fe^{2+} using H_2O_2, and determined the Fe^{2+} concentration as the difference between the two measurements. Our preliminary results demonstrate higher Fe^{2+} concentrations during glacial periods than during interglacial periods. This elevated concentration of Fe^{2+} suggests that more iron was available for phytoplankton growth during the Last Glacial Maximum, than would be expected from measurements of proxies such as dust mass or total Fe.

Introduction

Iron (Fe) is the fourth most abundant element in the Earth's crust (~5.6%)[1] and is primarily introduced into the oceans by dust deposition.[2] In the open ocean, Fe has a concentration between 0.05 and 2 nM,[3] with a typical nutrition profile.[4] Once deflated, dust aerosols have a typical atmospheric lifetime from hours to days[2] thus permitting their long-range global transport to all of the Earth's oceans.[5]

Iron plays an important role in phytoplankton metabolism[6] where it is essential for photosynthetic and respiratory electron transport.[7] The hypothesis that Fe can act as a limiting micronutrient in High-Nutrient Low-Chlorophyll (HNLC) regions[8] is now generally accepted and has been investigated[9] in HNLC areas of the Southern Ocean,[10] equatorial Pacific[11] and Subarctic Ocean.[12] The artificial addition of iron to equatorial Pacific Ocean waters (IronEx)[13] and the polar Southern Ocean (SOIREE)[14] resulted in significant increases in phytoplankton productivity and abundance.[11] The broader implication is that in HNLC waters, the presence of Fe can increase the efficiency of the biological pump, the process by which CO_2 fixed in photosynthesis is transferred to the deep ocean,[15] and promote drawdown of atmospheric carbon dioxide.[16]

Iron speciation and its relationship to phytoplankton growth have also been investigated from several perspectives, including the colloidal state of iron and its ability to form complexes with organic ligands.[17] Iron speciation is driven by a combination of factors including environmental conditions, rates of the chemical transformation, and the presence of organic and inorganic biomass and particulate matter.[18] Iron is present in the ocean as Fe (III) or Fe(II) species.[19] The ratio in seawater is strongly in favor of the Fe(III) species, with Fe(II)/Fe(III) values on the order of 10^{-10},[20] however, the ratio between unbound ions Fe^{2+}/Fe^{3+} is in favor of Fe^{2+} with a value of 2.63.[18] Iron in the open ocean is dominated by Fe(III) which predominately forms complexes with organic ligands, but Fe(II) is also present. Some studies demonstrate that

[a]*Department of Earth Science, University of Siena, Via Laterina 8, 53100 Siena, Italy*
[b]*Department of Environmental Sciences, Informatics and Statistics, University Ca' Foscari of Venice, Dorsoduro 2137, 30123 Venice, Italy. E-mail: barbante@unive.it; Fax: +39 041 2348549; Tel: +39 041 2348942*
[c]*Centre for Ice and Climate, Niels Bohr Institute, Juliane Maries Vej 30, 2100 Copenhagen, Denmark*
[d]*Institute for the Dynamics of Environmental Processes-CNR, University of Venice, Dorsoduro 2137, 30123 Venice, Italy*
[e]*Accademia Nazionale dei Lincei, "Centro Beniamino Segre", via della Lungara, 10 00165 Rome, Italy*
[f]*Laboratoire de Glaciologie et Géophysique de l'Environnement (UMR UJF/CNRS 5183), 54, rue Molière, Domaine Universitaire, B.P. 96, 38402 Saint Martin d' Hères, France*
† Electronic supplementary information (ESI) available. See DOI: 10.1039/c1ja10276a

Fe(II) species are more soluble than Fe(III),[21] with much of the variability in Fe solubility linked to changing concentrations of Fe (II) in dust[22] and for this reason varying bioavailability.[23] Thus, variations in dust deflation zones may contribute greatly to changes in bioavailability of Fe in the open ocean.

Polar ice caps are important sites for climate studies due to their ability to archive atmospheric constituents, the possibility for accurate sample dating, and their relative distance from anthropogenic pollution sources. Antarctic ice cores additionally offer the possibility to study a wide range of contemporaneous changes in atmospheric and ocean chemistry over several glacial–interglacial cycles.[24] Large glacial–interglacial changes in iron deposition have been determined from the iron flux in the EPICA Dome C ice core,[25] with the observation of a higher acid leachable iron fraction during glacial climate periods.[26] Kim *et al.*[27] investigated the formation of bioavailable iron from the dissolution of iron oxide particles in the ice phase under both UV and visible light irradiation.

Measurement of iron species is difficult due to high lability, reactivity and reversibility of the oxidation state of the species,[28] in addition to the potential for contamination during sample preparation and analysis. Separation of iron species can be achieved by pH-dependent retention of Fe(II) and Fe(III), by selective complexation of one species and subsequent separation, or by sorption of one of the species on a resin with subsequent elution. Coupled techniques, such as flow-injection chemiluminescence,[29] spectrophotometry,[30] atomic absorption spectrometry (AAS),[31] inductively coupled plasma-optical emission spectrometry/mass spectrometry (ICP-OES/MS),[32] cathodic stripping voltammetry[33] and fluorimetry,[34] are commonly used to quantify Fe(II) and Fe (III) species. ICP-MS is widely accepted for the study of trace elements in environmental matrices, but determination of ^{56}Fe at trace levels by this technique is complicated by the presence of polyatomic interfering ions such as $^{40}Ar^{16}O^{+}$ and $^{40}Ca^{16}O^{+}$.[35] The collision reaction cell (CRC) removes polyatomic interferences by their reaction or collision with a constant helium stream,[36,37] thus enabling the determination of ^{56}Fe by quadrupole-based ICP-MS.

The aim of this work is to investigate the speciation of Fe in ice from Talos Dome, Antarctica. Assuming that all of the iron present in Antarctic ice is derived from atmospheric dust deposition, this matrix should allow an evaluation of variations in Fe speciation since the Last Glacial Maximum (LGM) and consequent implications for ocean primary productivity. We concentrated on the instability of Fe(II) in oxidizing environments to the ppb (ng g^{-1}) concentrations of Fe present in Antarctic ice samples.[25] To address these challenges, we report a novel method coupling flow injection (FI) techniques with a collision reaction cell-inductively coupled plasma-mass spectrometry (CRC-ICP-MS). The novelty of the method relies on a considerably reduced number of reagents used, a decreased analysis time, and a special attention to sample handling procedures that minimize the potential for sample contamination at the very low concentrations of iron present in Antarctic ice.

Experimental

Sample location and preparation

Antarctic ice samples were obtained from sections of the Talos Dome (TD) ice core, drilled between 2005 and 2007. Talos Dome is an ice dome on the edge of the East Antarctic plateau, about 290 km from the Southern Ocean and 250 km from the Ross Sea.[38] The Talos Dome summit (159°04′21″E, 72°47′14″S, 2318.5 m a.s.l.) encompasses approximately 1880 m of ice, the deepest of which has been dated to 250 kyr before present (BP).[38] Featuring a mean annual temperature of −41 °C and an average accumulation rate of 80 mm water equivalent, the site is an excellent location for the long-term preservation of climatic signals of Southern Hemispheric climate change. Four samples obtained from Holocene ice strata (designated '*interglacial*') and two samples from LGM (Last Glacial Maximum) strata (designated '*glacial*') were analyzed. The TALDICE-1 sample chronology[39] was applied.

The ice cores were transported in a frozen state to the laboratory at the University of Venice and then cut to a suitable size for analysis (2 × 2 × 3 cm) using a modified commercial band saw with polyethylene tabletop and guides. The table, guides and saw were carefully cleaned with acetone and methanol to remove contamination before each use. Samples were decontaminated by immersion in a sequence of three different baths of Maxy system (La Garde, France) ultrapure water (UPW), guaranteeing the complete removal of surface contamination[40] with thorough rinsing between each immersion step. UPW was prepared from deionised water which was then purified by passing it through a mixed bed of ion exchange resins (Maxy, La Garde, France). For each bath, the water temperature was approximately 20 °C. Samples were immersed in the first bath for approximately 25 s with approximately 30% of the sample mass lost at this stage. In the second and third baths, samples were immersed for less time, approximately 15 s, with the total loss of a further 40% of the sample mass. The bath is changed every three samples to avoid any possible contaminations. At the end of the entire process the remaining mass of the sample was about one-third of the starting mass (about 5 mL remaining from 15 mL). The decontaminated frozen sample was acidified with 0.05 mL of 1 M nitric acid solution (obtaining a pH of 1.9) and kept frozen to minimize the possibility of Fe speciation artefacts.

Instrumentation

All reagents and standard solutions were prepared with ultra pure water (UPW, 18 MΩ cm^{-1}). Nitric acid (trace metal grade, Romil, Cambridge, UK) was diluted with UPW to make up a 1 M HNO_3 eluent. A carrier solution was then made by diluting the eluent solution to obtain a 0.02 M HNO_3 solution (pH 1.6). Analytical grade (SpA) H_2O_2 (Romil, Cambridge, UK) was used to oxidize the iron (according to de Jong, *et al.*[41]).

A flow injection (FI) manifold, shown in Fig. 1, coupled with an Agilent 7500cx series CRC-ICP-MS (Agilent, California, USA) (see ESI 1†), was used for Fe species determination. The CRC-ICP-MS was equipped with a Scott spray chamber, with instrument parameters reported in Table 1. The FI manifold consisted of two valves and a ten-channel peristaltic pump (Ismatec, Glattbrugg, CH) used to maintain a constant system flow rate of 0.8 mL min^{-1}. Fluid selection and handling were controlled by the combination of a 10-port injection valve (V_1) for sample loading and a 6-port selection valve (V_2) for reagent selection (both from Valco Instruments

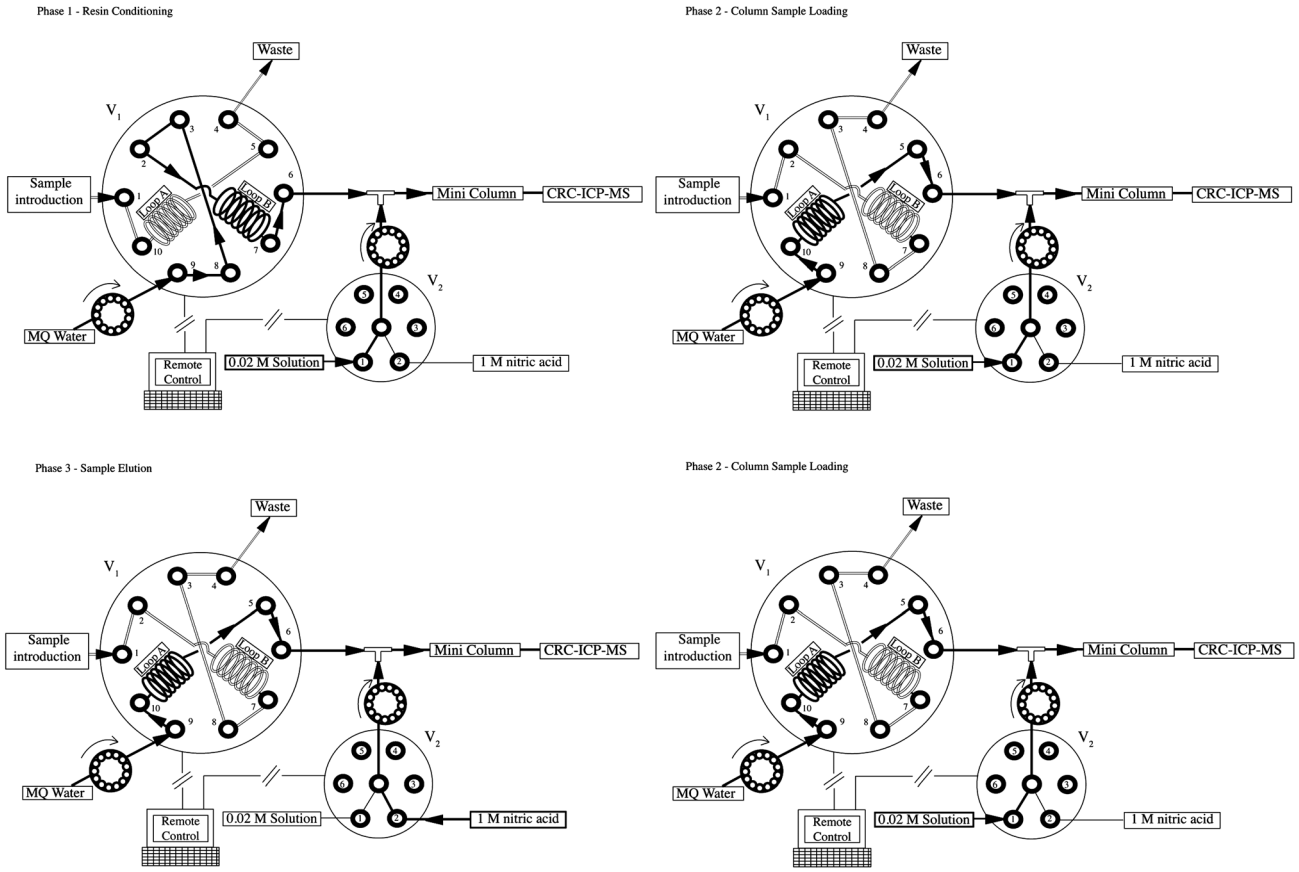

Fig. 1 Schematic view of the flow injection manifold system for sample introduction to the CRC-ICP-MS. Solid lines indicate the path of fluid transport through the system (0.8 mL min^{-1}) while the hollow lines show the sample loading channel.

Co. Inc., Houston, USA). Samples were first conditioned (0.02 M HNO_3 added *via* a T-junction), then injected into a sample loop (V_1 switch) and finally sent to the CRC-ICP-MS using a 1 M HNO_3 eluent (V_2 switch). V_1 consists of two sampling loops. Loop A (Fig. 1) continues to elute while samples are injected in loop B. Such a configuration is optimal for implementation in continuous flow analysis (CFA) systems of the type commonly used for ice core sampling.[42] The manifold inject/load cycles were controlled by a custom DOS-based program. The manifold was cleaned daily by passing through eluent solution for one hour.

Table 1 Instrumental parameters for CRC-ICP-MS

Plasma parameter		
	RF power	1500 W
	Sample depth	7.6 mm
	Coolant gas	15.0 L min^{-1}
	Plasma gas	0.75 L min^{-1}
	Carrier gas	1.20 L min^{-1}
	Optional gas	0%
	Nebulizer pump	0.05 rps
	S\C temp	2 °C
Ion lenses		
	Extract 1	0.2 V
	Extract 2	−121.0 V
	Omega–bias-ce	−24 V
	Omega–lens-ce	0.4 V
	Cell entrance	−32 V
	QP focus	−8 V
	Cell exit	−44 V
Q-Pole parameters		
	QP bias	−16.1 V
Octpole parameters		
	OctP RF	120 V
	OctP bias	−18.0 V
Reaction cell		
	H_2 gas	0 mL min^{-1}
	He gas	5.6 mL min^{-1}

All sampling tubing except for pump tubing was 0.75 mm i.d., PTFE tubing (Grace, Illinois, USA). The pump tubing utilized was either Tygon or PharMed tubing (Tygon for PTFE tubing connections and PharMed for the pump tubing) (Ismatec, Glattbrugg, CH). All connections were 1/4–28 low pressure Tefzel flangeless fittings (Valco Instruments Co. Inc., Houston, USA). The NTA Superflow resin (Qiagen Inc., Valencia, USA) was packed into a 2 cm Global-FIA mini-column (Global-FIA Inc., Fox Island, USA). The column consisted of a tapered inner chamber sealed with nonmetal frits. To minimize contamination, sample and reagent bottles were kept in double-sealed low density polyethylene (LDPE) bags within a HEPA-laminar class 100 airflow bench. Teflon tubing was passed through small holes from the bottles to the manifold, which was also situated within a HEPA environment. LDPE sample and reagent bottles (Nalgene, Rochester, USA) were rigorously cleaned with nitric acid following the procedures of Vallelonga, *et al.*[43]

Procedure

Decontaminated ice core samples were melted immediately before being loaded into the manifold in order to minimize any potential red-ox reactions. A heat source was used to melt the samples in approximately 60 s. The measurement procedure is as follows: immediately after melting of the 5 g ice sample, a 1 mL aliquot was loaded into sample loop A with a polypropylene syringe. The syringe was carefully cleaned with 1 M HNO_3 and UPW before each sample. After the loop was charged, valve V_1 switches position so that the sample can be loaded onto the resin. A sample acid correction is made with a second flux arriving in the T junction from V_2. The 0.02 M carrier solution, in accordance with de Jong *et al.*,[41] acidifies the sample to approximately pH 2 (an exit pH of 1.87 was measured) which is necessary for the retention of Fe^{3+} on the resin. At the same time, the remaining sample is loaded into loop B and, fully oxidized with the addition of 0.05 mL of UPA H_2O_2 (Romil, Cambridge, UK) to convert all Fe^{2+} to Fe^{3+}. When the sample has been loaded onto the resin, valve V_2 switches position so the 1 M HNO_3 eluent is passed through the resin. After elution, valve V_2 switches back to the carrier solution so the resin is conditioned for the next analysis. Following the initial measurement (of Fe^{3+}), valve V_1 switches to pass the oxidized sample from loop B through the resin and into the analytical system. The concentration of Fe^{2+} was determined as the difference between the integrated areas of two measured peaks. A single run requires 9 minutes while a complete sample measurement requires approximately 20 minutes.

Tests were carried out to optimize the sample volume to have the best detection limit without saturation of the resin. This problem became evident when analysing the external calibration curve standards. It was found that increasing the loop volume over 1 mL produced a faster saturation of the resin and consequently an incomplete retention of the standard. This caused a shift in the slope of the calibration curve. With a sample volume of 1 mL all of the Fe^{3+} present in the standards is reliably retained.

Results and discussion

Matrix effects and interference study

Although Antarctic ice is an extremely clean matrix with low elemental concentrations[24] the possibility of matrix effects were still investigated by conducting external calibration tests.[44] Two calibration curves were created where one used standards in a melted ice matrix while the other created an external calibration curve using acidified UPW. The ice matched and UPW standards were both acidified to pH 2 with nitric acid and were added with Fe^{3+} to span concentrations between 0.1 and 10 ng g^{-1}. A 4% difference between the calibration slopes was measured. The matrix-matched standards present a slope of 459 707 while external calibration standards have a slope of 477 774. We infer that the matrix effect is negligible. Both UPW and ice calibration curves had a correlation coefficient greater than 0.99 (d.f. = 3, 95% confidence intervals).

ArO^+ (mass = 56) is the abundant interfering ion for the major isotope of iron (^{56}Fe).[45] The ICP-MS fitted with a helium gas collision/reaction cell removes iron interferences without a complete signal loss.[45,46] Once ArO^+ is removed, ^{56}Fe can be measured with improved sensitivity and lower detection limits.[45] The $^{56}Fe\backslash^{57}Fe$ intensity ratio decreases from a value of 250 measured using a flux of 2 mL min^{-1} to 42 using a flux of 5.6 mL min^{-1} which is close to the natural ratio of 41.6.[47] The instrumental condition parameters are reported in Table 1.

Quantification

Ni-NTA Superflow resin is ideal for the study of Fe speciation because it is able to retain Fe^{3+} completely at pH 2 with no retention of Fe^{2+}.[48] As Fe speciation is driven principally by pH,[49] it is very important to maintain the sample pH close to 2 because all species of Fe(II) and Fe(III) are in the Fe^{3+} and Fe^{2+} free form.[19] The oxidation kinetics of Fe(II) to Fe(III) can be markedly slowed by acidification to pH near 3.[49] Thus any Fe(II) present in the original sample liberated at pH 3 or less would tend to be stabilized as Fe(II),[50] rather than oxidized to Fe(III).

Quantification of Fe^{3+} and Fe^{2+} was performed by external calibration curves where Fe^{3+} standards were prepared by diluting a 1000 mg L^{-1} stock solution (SPEX, US, plasma standard) in 0.02 M HNO_3 UPW solutions. No memory effects were present between analyses. Chromatographic data analysis software (Agilent, California, USA) was used for peak integration. Fe^{3+} quantification was obtained by peak integration before oxidation with H_2O_2 while Fe^{2+} has been quantified by difference between the areas of the oxidized and unoxidized samples. This technique of quantification of Fe^{2+} by difference is necessary because of problems associated with the direct quantification of the unretained Fe^{2+}. Firstly, the shape of the unretained Fe^{2+} peak is spread-out and hence poorly defined. Furthermore it is not only Fe^{2+} that passes through the resin at pH 2 but other organic and inorganic iron-bound species[48] which further inhibits the practicality of this method of Fe^{2+} quantification.

Blanks and detection limits

Considering the extremely low concentrations of iron in Antarctic ice, special care was taken to evaluate the procedural blanks. Procedural blanks were obtained by 3 repeat analyses of 1 mL aliquots of UPW acidified to 0.02 M with HNO_3 loaded in the loop and, using the gradient of the regression line, we calculated the concentration of iron in the UPW. The blank was determined to be 0.176 ± 0.004 (blank 1 0.172 ng mL^{-1}, blank 2 0.179 ng mL^{-1} and blank 3 0.177 ng mL^{-1}). The limit of detection (LOD), defined as 3 times the standard deviation of the procedural blank, was calculated to be 0.01 ng mL^{-1} for both Fe^{2+} and Fe^{3+}.

Fe^{2+} stability in UPW and Antarctic ice

Fe(II) species and in particular Fe^{2+} are rapidly oxidized by O_2 to the thermodynamically stable Fe(III) form.[51] Inorganic Fe(III) is extremely insoluble and precipitates eventually forming highly stable crystalline minerals that are not available for biological use[52] necessitating the evaluation of the stability of Fe^{2+}. Since we expected different concentrations between glacial and interglacial times we studied the oxidation kinetics at different concentrations. We prepared three standards with different concentrations of Fe^{2+} (1, 12 and 17 ng g^{-1}: STD1, STD2 and STD3, respectively) in a 0.02 M HNO_3 solution. The results

demonstrate that there is no appreciable difference in oxidation rate for different concentrations of Fe^{2+} (Fig. 2). In these UPW standards the half-life was calculated to be 250 minutes. Our results are on the same order of magnitude as previous studies: Zhuang *et al.*[21] determined a half-life of about 70 minutes, and Morgan *et al.*[49] found a strongly pH dependent half-life of about 100 minutes. Our results confirm the relative stability of Fe^{2+} at low pH, especially when considering the oxidation half-life of 3.5 min in seawater at pH 8.[53]

To verify the complete oxidation of Fe^{2+} after the addition of H_2O_2 we compared the addition of 0.05 mL of UpA H_2O_2 30 minutes before analysis (Fig. 2 black circles) to the addition of H_2O_2 immediately before analysis (Fig. 2 black asterisk). In both cases we find near-total oxidation of Fe^{2+} to Fe^{3+}. Therefore the oxidation procedure can be carried out immediately before analysis with the red-ox state maintained for at least a few hours (Fig. 2 black asterisks). We used a control standard (Fig. 2, hollow squares) to test the long-term behavior of Fe^{2+} over 34 hours. The oxidation half-life is therefore confirmed over a long period. The behavior of this standard further confirms Fe^{2+} oxidation is independent of concentration.

We then conducted a series of replicate measurements to evaluate if the Fe^{2+} oxidation proceeded at the same rate in a real ice matrix. A bulk ice sample was produced from melted glacial and interglacial ice. The sample was spiked with 0.91 ng g^{-1} Fe^{2+} prepared from $FeCl_2$ salt. Our results (Fig. 3) demonstrate that the sample oxidation rate is faster than in the UPW matrix, and has a half-life of approximately 70 minutes. This change could be due to the presence of metal and dust particles in the Antarctic ice matrix which may serve as catalysts.[49] As a final test the sample was oxidized with H_2O_2 to determine a Fe^{2+} recovery of 95% (Fig. 3, black circles). In our samples the Fe^{2+} was almost completely (95%) oxidized after 360 minutes.

Two glacial samples (dated to 16.2 ky BP and 19.7 ky BP) were prepared as described above and obtained from glacial ice strata, which contain greater concentrations of dust and impurities than interglacial ice.

The samples were analyzed to evaluate the stability of Fe^{2+} in solution. The results (Fig. 3) show two similar curves describing a faster oxidation rate than those observed for ice or UPW matrices. In this case, the half-life appears to be on the order of 20 to 30 minutes. However, for the first 15 minutes the Fe^{2+} seems stable or without appreciable variation (<20%), indicating that there is a sufficient period of time available to conduct the analysis after melting while avoiding an appreciable loss of Fe^{2+}. The slight difference between the two curves may be explained by the different ages of the samples, which likely feature different concentrations of dust, metals and ionic compound that could be able to modify the oxidation rate. Our results and those in the literature confirm that Fe^{2+} is an unstable species and consequently ice samples should be analyzed immediately after melting to avoid any loss of Fe^{2+}.

Recovery and precision

No certified reference materials are available for polar ice matrices, and particularly for speciated elements, to evaluate the accuracy and precision of their recovery. To test this, we analyzed a melted Antarctic sample spiked to different concentrations of Fe^{3+}. Three standards were prepared at concentrations of 0.15, 3.79 and 10.78 ng g^{-1} (Table 2). Using an external calibration curve made in an UPW matrix we calculated the recovery for the three prepared standards. The recovery for Fe^{3+} is consistently in the range of 96% to 100% (Table 2) in accordance with the results obtained by Lohan, *et al.*[48] Precision (Table 3) was tested by analyzing three samples cut and decontaminated using the methods described above for an individual ice core sample. It was not possible to melt and homogenize the samples due to the rapid oxidation of Fe^{2+}. A precision of 2% was obtained for total Fe (sum of Fe^{2+} and Fe^{3+}), 7% for Fe^{3+} and

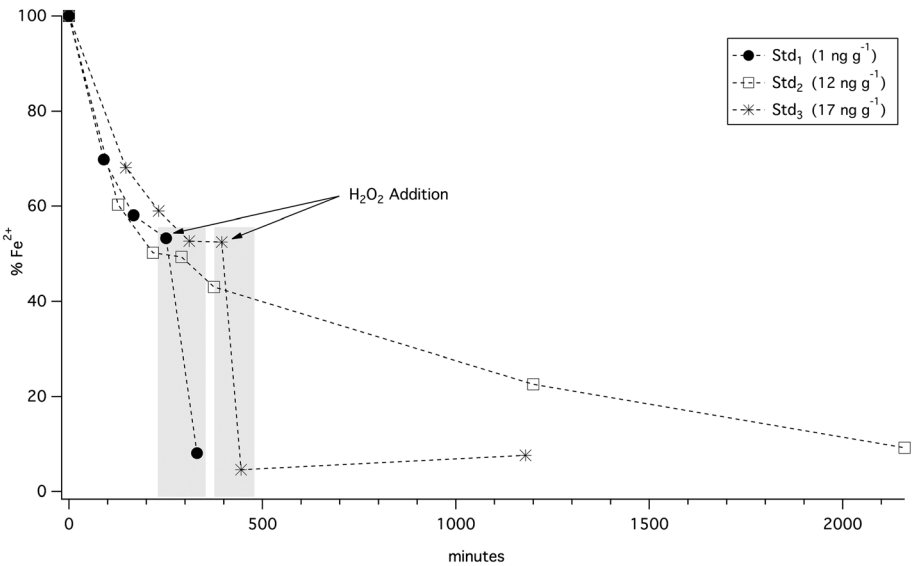

Fig. 2 Fe^{2+} oxidation rate in an ultra pure water matrix acidified to pH 2. The oxidation rate of Fe^{2+} is similar for different Fe concentrations. The light grey bars highlight the effect of oxidation by H_2O_2 addition.

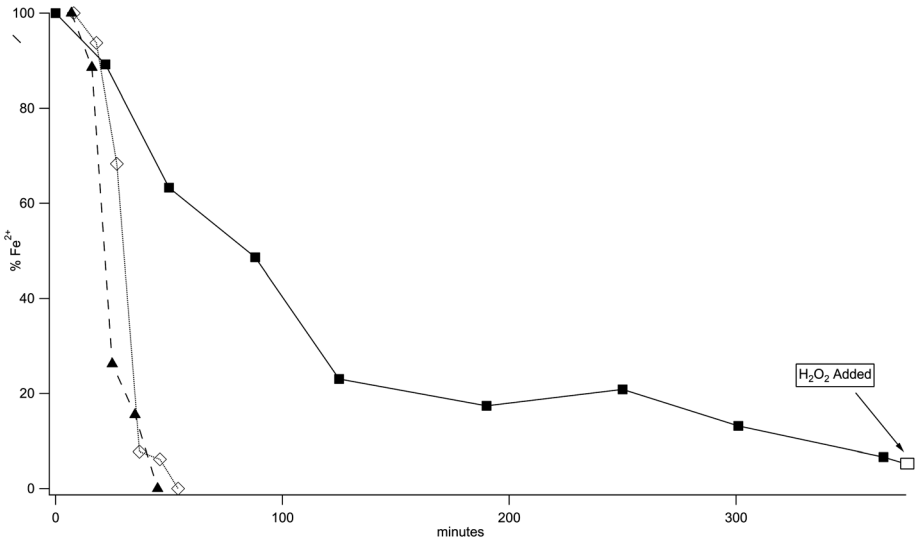

Fig. 3 Oxidation rate of Fe^{2+} added to a refrozen Antarctic ice matrix acidified to pH 2. Black squares represent the oxidation rate while white squares show the percentage of Fe^{2+} remaining 365 minutes after oxidation by H_2O_2 addition. Oxidation of Fe^{2+} is also shown in Antarctic Talos Dome samples dated to 16.2 ky BP (black triangles) and 19.7 ky BP (white circles).

Table 2 Recovery of Fe^{3+} in an Antarctic ice matrix

	Fe^{3+} added/ng mL^{-1}	Fe^{3+} determined/ng mL^{-1}	%Recovery
Spike 1	0.15	0.15 ± 0.01	100
Spike 2	3.79	3.64 ± 0.25	96
Spike 3	10.78	10.58 ± 0.61	98

Table 3 Measurement precision evaluated from the determination of Fe species in three samples obtained from an Antarctic ice core sample

Sample	Fe^{3+}/ng mL^{-1}	Fe^{2+}/ng mL^{-1}	$(Fe^{3+} + Fe^{2+})$/ng mL^{-1}
Sample 1	1.09	0.34	1.42
Sample 2	1.24	0.21	1.46
Sample 3	1.17	0.31	1.48
Average	1.16	0.29	1.45
RSD	0.08	0.06	0.03
RSD%	6.9	22	2.1

22% for Fe^{2+}, demonstrating the instability of Fe^{2+}. In the absence of a suitable reference material, the accuracy was evaluated by adding a known concentration of Fe^{2+} obtained from a diluted solution of $FeCl_2$ salt (J.T. Baker, Griesheim, Germany) to a melted ice sample. First 0.51 ng g^{-1} was added to a mixed interglacial–glacial sample, which was then immediately frozen in liquid nitrogen (−196 °C) and placed in a cold room at a temperature of −20 °C for about three hours. The sample was then melted in 60 s with a heat source and immediately analyzed. The obtained recovery using this technique was 83% (0.44 ng g^{-1}).

Comparison with literature methods

Here Ni-NTA Superflow resin is used to isolate iron species, showing great efficiency in preconcentration and recovery of iron. We have described a novel technique which is capable of determining Fe species at trace concentrations with minimal sample handling and requiring few reagents that can be obtain at a very high purity grade. By comparison, all of the procedures found in the literature describe separate preconcentration and analytical stages (with two[48] or more[54] steps) often requiring greater numbers and volumes of reagents. These methods are summarised here:

Lohan, *et al.*[48] use acetic acid/ammonium buffer for conditioning Ni-NTA Superflow resin, 6 N HCl or 50% (v/v) NH_4OH to adjust the pH of the sample, ammonium acetate and Milli-Q water for rinsing and 0.5 N HNO_3 for eluting. The metals eluted from the resin were collected in 7 mL high density polyethylene (HDPE) vials and only subsequently analysed by SFMS-ICP-MS.

Spectrophotometric determination has been applied to on-line iron speciation analyses but requires a greater number of solutions with respect to the method proposed here. For example, Blain and Trèguer[55] determined Fe species with detection limits of 0.02 ng g^{-1} but requiring the use of ascorbic acid, methanol, 0.7 M NaCl, 2.5 M buffer solution (sodium acetate, acetic acid, pH 4.5) and 10^{-3} M ferrozine neocuprine.

Xiong, *et al.*[32] proposed a method using Electro Thermal Vaporization (ETV-ICP-OES) with a detection limit of 0.05 ng g^{-1} but this required the 156 times preconcentration of a 17 mL sample, in addition to the use of a greater number of reagents.

Cathodic stripping voltammetry (CSV) has been extensively used for the chemical speciation of iron in seawater. The CSV method allows very low detection limits (on the order of low pg g^{-1}) but the main disadvantages of this technique are long equilibration times as well as the presence of competing ligands.[56]

Ice core samples

Six ice core samples were analyzed: four from the current interglacial period and two from the last glacial climatic period (Table 4). These samples demonstrate appreciable differences in iron speciation. Interglacial Fe^{3+} concentrations have an average

Table 4 Concentrations of Fe^{3+} and Fe^{2+} determined in samples from the Antarctic Talos Dome ice core

Sample code	Sample age/ybp	Fe^{3+}/ng mL^{-1}	Fe^{2+}/ng mL^{-1}	(Fe^{3+} + Fe^{2+})/ng mL^{-1}	Fe^{2+}/Fe^{3+}
103	1024	0.36 ± 0.02	0.05 ± 0.01	0.41 ± 0.01	0.14
176	1997	0.30 ± 0.02	0.01 ± 0.01	0.31 ± 0.01	0.05
403	5622	0.30 ± 0.02	0.05 ± 0.01	0.35 ± 0.01	0.16
427	6089	0.19 ± 0.01	0.15 ± 0.03	0.33 ± 0.01	0.79
850	19 719	1.24 ± 0.09	0.51 ± 0.11	1.75 ± 0.04	0.41
965	31 613	0.71 ± 0.05	0.32 ± 0.07	1.02 ± 0.02	0.45

value of 0.29 ng g^{-1} while mean glacial concentrations are 0.97 ng g^{-1}. The same behavior is evident for Fe^{2+}, which presents lower concentrations during the interglacial period (average of 0.07 ng g^{-1}) and greater values during the glacial period (average of 0.41 ng g^{-1}). This variation in both species may be attributed to higher iron fluxes[24] over Antarctica during the glacial period. An interesting feature of the data is that the Fe^{2+}/Fe^{3+} ratio decreases from glacial to interglacial climate, indicating a reduction in the relative abundance of Fe^{2+} since the glacial period. The greater concentrations of Fe^{2+} found in glacial samples may have important repercussions for past variations in the strength of the biological pump in the Southern Ocean. A reduction in Fe^{2+} at the end of the glacial period agrees with the hypothesis[8] of a reduced biological pump at the initiation of the current interglacial climate. This is the first work to demonstrate that the speciation of Fe deposited in Antarctica, and hence over the Southern Ocean, changed between the glacial and interglacial periods. The greater contribution of more readily bioavailable Fe^{2+} to the Southern Ocean during the glacial period may have increased the efficacy of the biological pump and hence the sequestration of atmospheric CO_2. These initial results allow only a preliminary evaluation of the role of iron fertilization in glacial–interglacial climate dynamics, but they do provide a fundamental confirmation of the principal processes.

Conclusion

In this paper we present a rapid, low-contamination method for determining iron speciation in a polar ice core matrix. Contamination control is fundamental to accurately determine Fe concentrations in such a pure matrix. The complete automation of the methods and the few reagents required, only 1 M HNO_3 eluent and 0.02 M HNO_3 conditioning solution, further reduce the risk of sample contamination. The high sensitivity and robustness of the CRC-ICP-MS detector system permit low detection limits comparable with most previous work but with a shorter analysis time. Particular attention has been given to the stability of Fe^{2+} in pure water and polar ice matrices. Our findings support the contention that variations in Fe^{2+} oxidation kinetics are related to impurities in the sample matrix.

In freshly melted Antarctic ice we found faster oxidation rates compared to purified laboratory waters. This behaviour could be explained by the catalysing effect of ions such as Co^{2+} and Cu^{2+}, elements which are present in the ice core and could greatly enhance the oxidation rate.[49] The presence of these elements cannot explain the differences in oxidation rate observed after the melted ice has been kept for longer periods of time, since the ice still contains the same concentrations of metals. This phenomenon may be possibly explained by the dissolution of carbonate in the ice. The concentration of carbonate in freshly melted ice is much lower due to the time necessary for dissolved carbonate in the sample to equilibrate with atmospheric CO_2.

The slower oxidation rate was detected in the UPW probably due to the lower concentrations of elements compared to the ice matrix. The catalytic effect of copper and cobalt is less while the presence of carbonate could, together with the low pH value,[50] increase the stability of Fe^{2+}.

Acidification of the sample to pH 2 is not sufficient to completely stabilize the iron system but permits the melting and analysis of the sample without an appreciable loss of Fe^{2+} (recovery: 83%). The results obtained in Antarctic ice core samples indicate an increase in Fe^{2+} concentrations during glacial periods with respect to the present interglacial period. These results provide a preliminary demonstration of changing iron speciation between glacial and interglacial deposition over Antarctica.

Acknowledgements

This work was supported by University of Siena and IDPA-CNR (Institute for the Dynamics of Environmental Processes, National Research Council). PV acknowledges the support of an EU Marie Curie IIF Fellowship (MIF1-CT-2006-039529, TDI-COSO). We thank all colleagues in the University of Venice Environmental Analytical Chemistry Laboratory for instrumental assistance, technical information and English corrections. Roberto Zuliani is especially thanked for technical assistance and development of the software used for the manifold control. The Talos Dome Ice core Project (TALDICE), a joint European programme, is funded by national contributions from Italy, France, Germany, Switzerland and the United Kingdom. Primary logistical support was provided by PNRA at Talos Dome. This is TALDICE publication number 14. This work was supported by funding to the Past4Future project from the European Commission's 7th Framework Programme, grant number 243908, and is Past4Future contribution number 13.

References

1 E. P. Achterberg, T. W. Holland, A. R. Bowie, R. F. C. Mantoura and P. J. Worsfold, *Anal. Chim. Acta*, 2001, **442**, 1–14.
2 T. D. Jickells, Z. S. An, K. K. Andersen, A. R. Baker, G. Bergametti, N. Brooks, J. J. Cao, P. W. Boyd, R. A. Duce, K. A. Hunter, H. Kawahata, N. Kubilay, J. laRoche, P. S. Liss, N. Mahowald, J. M. Prospero, A. J. Ridgwell, I. Tegen and R. Torres, *Science*, 2005, **308**, 67–71.
3 K. W. Bruland, K. J. Orians and J. P. Cowen, *Geochim. Cosmochim. Acta*, 1994, **58**, 3171–3182.

4 K. W. Bruland, *Geochim. Cosmochim. Acta*, 2005, **69**, A1.
5 J. M. Prospero, P. Ginoux, O. Torres, S. E. Nicholson and T. E. Gill, *Rev. Geophys.*, 2002, **40**, 1002–1033.
6 K. W. Bruland, *Abstr. Pap., Jt. Conf. - Chem. Inst. Can. Am. Chem. Soc.*, 2000, **219**, U866.
7 W. G. Sunda and S. A. Huntsman, *Mar. Chem.*, 1995, **50**, 189–206.
8 J. H. Martin and S. E. Fitzwater, *Nature*, 1988, **331**, 341–343.
9 H. Planquette, P. J. Statham, G. R. Fones, M. A. Charette, C. M. Moore, I. Salter, F. H. NÈdÈlec, S. L. Taylor, M. French, A. R. Baker, N. Mahowald and T. D. Jickells, *Deep-Sea Res., Part II*, 2007, **54**, 1999–2019.
10 D. C. E. Bakker, A. J. Watson and C. S. Law, *Deep-Sea Res., Part II*, 2001, **48**, 2483–2507.
11 K. H. Coale, K. S. Johnson, S. E. Fitzwater, R. M. Gordon, S. Tanner, F. P. Chavez, L. Ferioli, C. Sakamoto, P. Rogers, F. Millero, P. Steinberg, P. Nightingale, D. Cooper, W. P. Cochlan, M. R. Landry, J. Constantinou, G. Rollwagen, A. Trasvina and R. Kudela, *Nature*, 1996, **383**, 495–501.
12 J. H. Martin and S. E. Fitzwater, *Nature*, 1988, 331.
13 K. H. Coale, K. S. Johnson, S. E. Fitzwater, S. P. G. Blain, T. P. Stanton and T. L. Coley, *Deep-Sea Res., Part II*, 1998, **45**, 919–945.
14 P. W. Boyd, A. J. Watson, C. S. Law, E. R. Abraham, T. Trull, R. Murdoch, D. C. E. Bakker, A. R. Bowie, K. O. Buesseler, H. Chang, M. Charette, P. Croot, K. Downing, R. Frew, M. Gall, M. Hadfield, J. Hall, M. Harvey, G. Jameson, J. LaRoche, M. Liddicoat, R. Ling, M. T. Maldonado, R. M. McKay, S. Nodder, S. Pickmere, R. Pridmore, S. Rintoul, K. Safi, P. Sutton, R. Strzepek, K. Tanneberger, S. Turner, A. Waite and J. Zeldis, *Nature*, 2000, **407**, 695–702.
15 W. G. Sunda, *Science*, 2010, **327**, 654–655.
16 P. W. Boyd, C. S. Law, C. S. Wong, Y. Nojiri, A. Tsuda, M. Levasseur, S. Takeda, R. Rivkin, P. J. Harrison, R. Strzepek, J. Gower, R. M. McKay, E. Abraham, M. Arychuk, J. Barwell-Clarke, W. Crawford, D. Crawford, M. Hale, K. Harada, K. Johnson, H. Kiyosawa, I. Kudo, A. Marchetti, W. Miller, J. Needoba, J. Nishioka, H. Ogawa, J. Page, M. Robert, H. Saito, A. Sastri, N. Sherry, T. Soutar, N. Sutherland, Y. Taira, F. Whitney, S.-K. E. Wong and T. Yoshimura, *Nature*, 2004, **428**, 549–553.
17 H. Obata, H. Karatani, M. Matsui and E. Nakayama, *Mar. Chem.*, 1997, **56**, 97–106.
18 H. J. W. De Baar and J. T. M. D. Jong, *Distributions, Sources and Sinks of Iron in Seawater*, 2001.
19 F. J. Millero, W. S. Yao and J. Aicher, *Mar. Chem.*, 1995, **50**, 21–39.
20 F. J. Millero, W. Yao and J. Aicher, *Mar. Chem.*, 1995, **50**, 21–39.
21 G. Zhuang, Z. Yi and G. T. Wallace, *Mar. Chem.*, 1995, **50**, 41–50.
22 J. M. Trapp, F. J. Millero and J. M. Prospero, *Geochem., Geophys., Geosyst.*, 2010, **11**, Q03014.
23 R. J. M. Hudson and F. M. M. Morel, *Proceedings of the Abstract of the 198th American Chemical Society National Meeting*, American Chemical Society, Washington, vol. 198, p. 99.
24 E. Wolff, C. Barbante, S. Becagli, M. Bigler, C. Boutron, E. Castellano, M. De Angelis, U. Federer, H. Fischer and F. Fundel, *Quat. Sci. Rev.*, 2010, **29**, 285–295.
25 E. W. Wolff, H. Fischer, F. Fundel, U. Ruth, B. Twarloh, G. C. Littot, R. Mulvaney, R. Rothlisberger, M. de Angelis, C. F. Boutron, M. Hansson, U. Jonsell, M. A. Hutterli, F. Lambert, P. Kaufmann, B. Stauffer, T. F. Stocker, J. P. Steffensen, M. Bigler, M. L. Siggaard-Andersen, R. Udisti, S. Becagli, E. Castellano, M. Severi, D. Wagenbach, C. Barbante, P. Gabrielli and V. Gaspari, *Nature*, 2006, **440**, 491–496.
26 V. Gaspari, C. Barbante, G. Cozzi, P. Cescon, C. F. Boutron, P. Gabrielli, G. Capodaglio, C. Ferrari, J. R. Petit and B. Delmonte, *Geophys. Res. Lett.*, 2006, **33**, L03704.
27 K. Kim, W. Choi, M. R. Hoffmann, H.-I. Yoon and B.-K. Park, *Environ. Sci. Technol.*, 2010, **44**, 4142–4148.
28 P. Pohl and B. Prusisz, *TrAC, Trends Anal. Chem.*, 2006, **25**, 909–916.
29 V. A. Elrod, W. M. Berelson, K. H. Coale and K. S. Johnson, *Geophys. Res. Lett.*, 2004, **31**, L12307.
30 R. J. Kieber, B. Peake, J. D. Willey and B. Jacobs, *Atmos. Environ.*, 2001, **35**, 6041–6048.
31 G. Weber, *Fresenius' J. Anal. Chem.*, 1991, **340**, 161–165.
32 C. Xiong, Z. Jiang and B. Hu, *Anal. Chim. Acta*, 2006, **559**, 113–119.
33 M. Gledhill and C. M. G. van den Berg, *Mar. Chem.*, 1994, **47**, 41–54.
34 P. Hoffmann, A. N. Dedik, J. Ensling, S. Weinbruch, S. Weber, T. Sinner, P. G,tlich and H. M. Ortner, *J. Aerosol Sci.*, 1996, **27**, 325–337.
35 M. Segura, Y. Madrid and C. Camara, *J. Anal. At. Spectrom.*, 2003, **18**, 1103–1108.
36 I. Feldmann, N. Jakubowski and D. Stuewer, *Fresenius J. Anal. Chem.*, 1999, **365**, 415–421.
37 Y. Takaku, T. Hayashi, I. Ota, H. Hasegawa and S. Ueda, *Anal. Sci.*, 2004, **20**, 1025–1028.
38 M. Frezzotti, G. Bitelli, P. de Michelis, A. Deponti, A. Forieri, S. Gandolfi, V. Maggi, F. Mancini, F. Remy and I. Tabacco, *Ann. Glaciol.*, 2004, **39**, 423–432.
39 D. Buiron, J. Chappellaz, B. Stenni, M. Frezzotti, M. Baumgartner, E. Capron, A. Landais, B. Lemieux-Dudon, V. Masson-Delmotte and M. Montagnat, *Clim. Past. Discuss.*, 2010, **6**, 1733–1776.
40 U. Ruth, C. Barbante, M. Bigler, B. Delmonte, H. Fischer, P. Gabrielli, V. Gaspari, P. Kaufmann, F. Lambert and V. Maggi, *Environ. Sci. Technol.*, 2008, **42**, 5675–5681.
41 J. de Jong, V. Schoemann, D. Lannuzel, J.-L. Tison and N. Mattielli, *Anal. Chim. Acta*, 2008, **623**, 126–139.
42 J. Gabrieli, P. Vallelonga, G. Cozzi, P. Gabrielli, A. Gambaro, M. Sigl, F. Decet, M. Schwikowski, H. Gäggeler and C. Boutron, *Environ. Sci. Technol.*, 2010, **44**, 3260–3266.
43 P. Vallelonga, K. Van de Velde, J. P. Candelone, C. Ly, K. J. R. Rosman, C. F. Boutron, V. I. Morgan and D. J. Mackey, *Anal. Chim. Acta*, 2002, **453**, 1–12.
44 C. Turetta, G. Cozzi, C. Barbante, G. Capodaglio and P. Cescon, *Anal. Bioanal. Chem.*, 2004, **380**, 258–268.
45 M. Iglesias, N. Gilon, E. Poussel and J.-M. Mermet, *J. Anal. At. Spectrom.*, 2002, **17**, 1240–1247.
46 M. Tanoshima and N. Sugiyama, *Presented in Part at the Winter Conference on Plasma Spectrochemistry 2010*, Fort Myers, Florida, 2010.
47 J. Eagles, S. J. Fairweather-Tait and R. Self, *Anal. Chem.*, 1985, **57**, 469–471.
48 M. C. Lohan, A. M. Aguilar-Islas, R. P. Franks and K. W. Bruland, *Anal. Chim. Acta*, 2005, **530**, 121–129.
49 B. Morgan and O. Lahav, *Chemosphere*, 2007, **68**, 2080–2084.
50 E. L. R. K. W. Bruland, in *IUPAC Series on Analytical and Physical Chemistry of Environmental Systems*, ed. D. R. Turner and K. A. Hunter, 2001, Wiley, Chichester, pp. 255–290.
51 H. Filik, B. D. Ozturk, M. Dogutan, G. Gumus and R. a. Apak, *Talanta*, 1997, **44**, 877–884.
52 H. W. Rich and F. M. M. Morel, *Limnol. Oceanogr.*, 1990, **35**, 652–662.
53 A. L. Rose and T. D. Waite, *Environ. Sci. Technol.*, 2002, **36**, 433–444.
54 M. Ozturk, E. Steinnes and E. Sakshaug, *Estuarine, Coastal Shelf Sci.*, 2002, **55**, 197–212.
55 S. Blain and P. Trèguer, *Anal. Chim. Acta*, 1995, **308**, 425–432.
56 C. M. G. van den Berg, *Anal. Chem.*, 2005, **78**, 156–163.